Bioorganic & Medicinal Chemistry Letters 19 (2009) 2006–2008

Contents lists available at ScienceDirect

Bioorganic & Medicinal Chemistry Letters

journal homepage: www.elsevier.com/locate/bmcl

Discovery of [3-(4,5,7-trifluoro-benzothiazol-2-ylmethyl)-pyrrolo[2,3-*b*] pyridin-1-yl]acetic acids as highly potent and selective inhibitors of aldose reductase for treatment of chronic diabetic complications

Michael C. Van Zandt [a,*], Brian Doan [a], Diane R. Sawicki [a], Janet Sredy [a], Alberto D. Podjarny [b]

[a] *The Institute for Diabetes Discovery, LLC, 23 Business Park Drive, Branford, CT 06405, USA*
[b] *Département de Biologie Structurale et Génomique, IGBMC, CNRS, INSERM, UDS, 1 rue Laurent Fries, BP 10142, 67404 Illkirch CEDEX, France*

ARTICLE INFO

Article history:
Received 26 November 2008
Revised 5 February 2009
Accepted 9 February 2009
Available online 12 February 2009

Keywords:
Aldose reductase
Aldehyde reductase
Diabetes

ABSTRACT

Efforts to identify treatments for chronic diabetic complications have resulted in the discovery of a novel series of highly potent and selective [3-(4,5,7-trifluoro-benzothiazol-2-ylmethyl)-pyrrolo[2,3-*b*]pyridin-1-yl]acetic acid aldose reductase inhibitors. The lead candidate, [6-methyl-3-(4,5,7-trifluoro-benzothiazol-2-ylmethyl)-pyrrolo[2,3-*b*]pyridin-1-yl]acetic acid example 16, inhibits aldose reductase with an IC50 of 8 nM, while being inactive against aldehyde reductase (IC50 > 100 μM), a related enzyme involved in the detoxification of reactive aldehydes.

Chronic diabetic complications which include blindness, renal failure, neuropathy, limb amputation, myocardial infarction and stroke arise from elevated levels of glucose in tissues such as the nerve, kidney, retina and lens. Although glucose is preferentially metabolized through the glycolytic pathway, during conditions of hyperglycemia, as observed in diabetes mellitus, elevated blood glucose levels saturate the normal pathways of glucose metabolism and a dramatic increase in flux through the polyol pathway results (Scheme 1).[1] Glucose entering the polyol pathway is reduced to sorbitol by aldose reductase (ALR2) and NADPH. Sorbitol is subsequently oxidized to fructose by sorbitol dehydrogenase and NAD^+. This increased flux through the polyol pathway results in a reduced ratio of NADPH to $NADP^+$, and an increased ratio of NADH to NAD^+. These changes, which alter the reduction potential of the cell are collectively termed oxidative stress. The impact of oxidative stress has been clearly demonstrated.[2] It is linked to depleted intracellular levels of reduced glutathione, increased non-enzymatic glycation and activation of protein kinase C.

Although many potent aldose reductase inhibitors (ARIs) have been identified and developed, none are currently marketed for worldwide use.[3] Many of these candidates failed to gain acceptance due to an inadequate therapeutic index.[4] In some cases this toxicity likely resulted from a lack of selectivity relative to aldehyde reductase (ALR1). The physiological importance of ALR1 has been clearly demonstrated.[5] It converts highly reactive 2-oxoaldehydes like 3-deoxyglucosone and methyl glyoxal to their corresponding nonreactive alcohols.[6] These aldehydes, which are involved in the formation of various protein cross-links and other advanced glycation end products (AGEs), are formed as degradation products from glucose and fructose.[7] During conditions of prolonged hyperglycemia, high concentrations of these aldehydes are formed resulting in the development of chronic diabetic complications and accelerated aging.[8]

As a member of the aldo-ketoreductase super family, ALR1 shares greater than 85% sequence homology with ALR2. Specific amino acid changes in the C-terminal loop, a section of the protein lining the active site cleft known as the specificity pocket, are primarily responsible for the various substrate and inhibitor specificities.[9]

Our work in this area has focused on identifying new carboxylic acid-based templates with significantly improved oral efficacy and selectivity relative to aldehyde reductase. Following the identification and clinical development of lidorestat (**1**, Fig. 1),[10] continued optimization of this series has resulted in the discovery of a novel series of [3-(4,5,7-trifluoro-benzothiazol-2-ylmethyl)-pyrrolo[2,3-*b*]pyridin-1-yl]acetic acids.

The target compounds were synthesized using the method illustrated in Scheme 2. The synthesis of [6-ethyl-3-(4,5,7-trifluoro-benzothiazol-2-ylmethyl)-pyrrolo[2,3-*b*]pyridin-1-yl]acetic acid (**15**) is described as an example. Here, acylation of 2-amino-6-ethylpyridine **2** with pivaloyl chloride gives the corresponding amide **3** in 54% yield after recrystallization. Subsequent treatment with 2 equiv of *tert*-butyl lithium followed by alkylation with methyl iodide gives 3-methyl substituted pyridine **4**. Retreatment with *tert*-butyl lithium provides the bis-anion which, after quenching with dimeth-

* Corresponding author. Tel.: +1 203 315 5951; fax: +1 203 488 3042.
E-mail address: michael.vanzandt@ipd-discovery.com (M.C. Van Zandt).

0960-894X/$ - see front matter © 2009 Elsevier Ltd. All rights reserved.
doi:10.1016/j.bmcl.2009.02.037

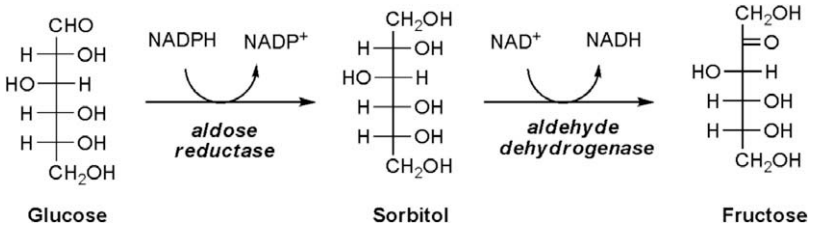

Scheme 1. Polyol pathway.

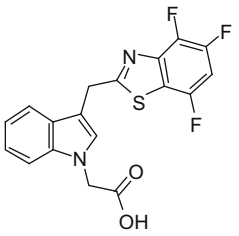

Figure 1. Lidorestat.

ylformamide and hydrolysis, gives the intermediate aldehyde. Without purification, cyclization with 4 N hydrochloric acid gives the desired 7-azaindole **5** in 58% yield (2 steps). Formation of gramine intermediate **6** with aq dimethylamine and formaldehyde in acetic acid followed by displacement with potassium cyanide in acetic acid gives indole-3-acetonitrile derivative **7**. Alkylation with ethyl bromoacetate using sodium hydride in acetonitrile provides the N-alkylated product (**8**) in 55% yield. In parallel, the 2-aminothiophenol hydrochloride salt **13** is prepared from 2,3,5,6-tetrafluoroaniline **9**. Acylation with acetic anhydride in pyridine at 120 °C followed by treatment with P_4S_{10} in benzene conveniently gives the intermediate thioamide **11**. Subsequent cyclization using sodium hydride provides 2-methylbenzthiazole **12**. Hydrolysis of the heterocyclic ring with aqueous sodium hydroxide followed by acidification with 2 N HCl gives the desired 2-aminothiophenol as the hydrochloride salt (**13**). Condensation with 7-azaindole 3-acetonitrile **8** as a melt provides benzothiazole **14** in 86% yield. Finally, hydrolysis with aq NaOH in ethanol provides the target compound **15** in 5% overall yield (9 linear steps).

With lidorestat proceeding to a phase II clinical trial, the major objective of this program has been to identify a highly potent and efficacious back-up candidate with increased selectivity. All compounds in the program were initially tested for potency against human aldose reductase (hALR2) and selectivity relative to human aldehyde reductase (hALR1). The results from these experiments are listed in Table 1.

Based on our experience with lidorestat and related carboxylic acid based aldose reductase inhibitors[9], the previously optimized 4,5,7-trifluorobenzthiazole side-chain which interacts directly with the specificity pocket[11] was kept constant while variations in the indole core were explored.

As illustrated in Table 1, the 7-aza-analogs are very potent and selective relative to ALR1. Example (**17**), along with the 6′-methyl (**16**) and 6′-ethyl (**15**) substituted compounds have IC_{50}'s of 7, 8 and 12 nM respectively. Activity for ALR1 is minimal with all compounds having IC_{50}'s > 100 μM.

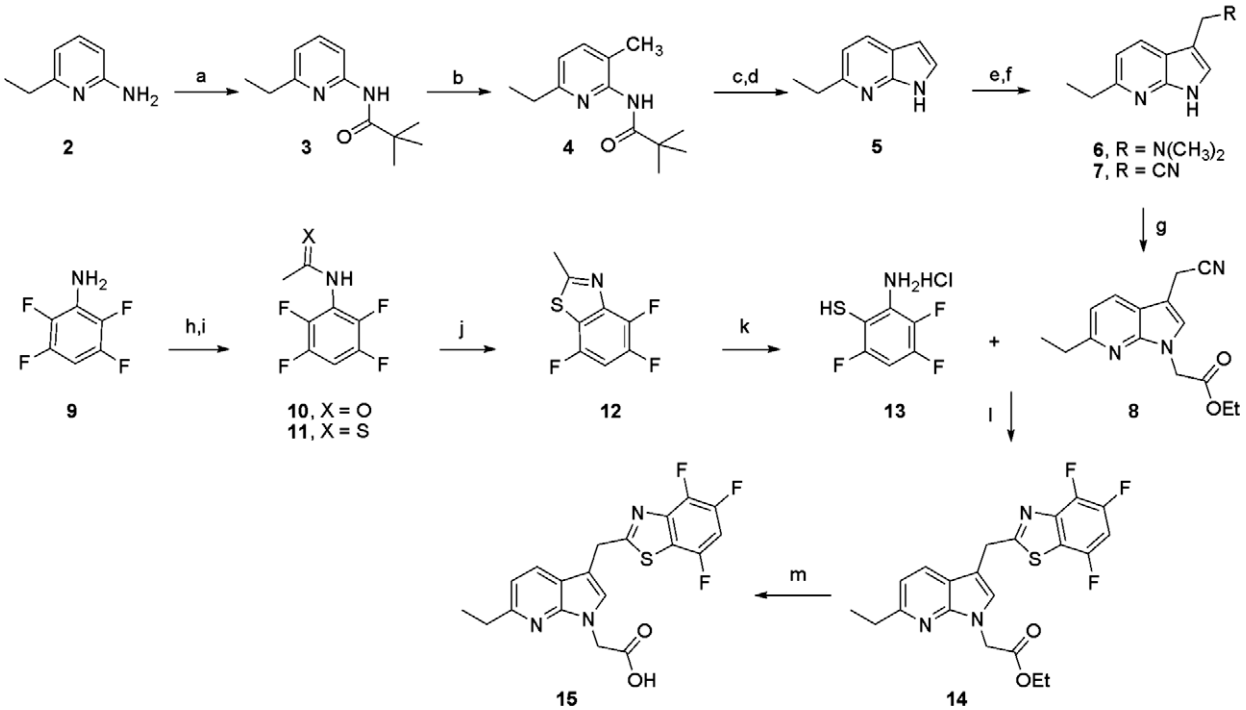

Scheme 2. Reagents and conditions: (a) PivCl, Et_3N, CH_2Cl_2, (54%); (b) (i) *t*-BuLi, (ii) MeI (69%); (c) (i) *t*-BuLi, THF; (ii) DMF; (d) 6 N HCl (58% c and d); (e) 40 wt % dimethylamine, 37 wt % formaldehyde, acetic acid, 100 °C (88%); (f) KCN, aq acetic acid, 110 °C (93%); (g) ethyl bromoacetate, NaH, acetonitrile (55%); (h) Ac_2O, pyridine, 120 °C (82%); (i)P_4S_{10}, benzene (88%); (j) NaH, toluene (96%); (k) 30% aq NaOH, ethylene glycol, 125 °C (73%); (l) melt, cat. BHT, 120 °C (86%); (m) aq NaOH, ethanol (56%).

Table 1
In vitro activity of 7-azaindoleacetic acid ARIs

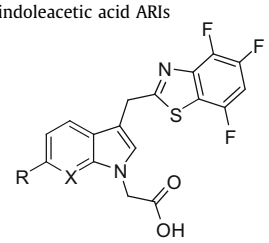

Ex.	R	X	hALR2[a] (nM)	HALR1[b] (nM)
1	H	CH	5	27,000
17	H	N	7	>100,000[c]
16	CH_3	N	8	>100,000
15	CH_2CH_3	N	12	>100,000

[a] Recombinant human aldose reductase.
[b] Recombinant human aldehyde reductase.
[c] %Inhibition < 50% @ 100,000 μM.

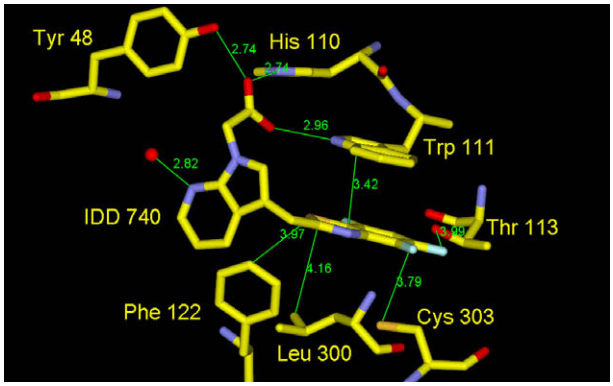

Figure 2.

The use of X-ray crystallography early in the program was essential. The structures provided a clear understanding of the important interactions that make up the enzyme-inhibitor complexes. The complexes were obtained using human ALR2 expressed in *Escherichia Coli* and crystallized with the oxidized form of the coenzyme β-NADPH$^+$ at pH 5 and 277 K. Diffraction data for example **17** was collected with a laboratory source at a resolution of 1.8 Å. As illustrated in Figure 2, the inhibitor is oriented in the active site of ALR2 in a manner such that the hydrophilic carboxylate head forms tight hydrogen bonds with the OH of Tyr 48 (2.74 Å), the NE2 of His 110 (2.74 Å) and the NE1 of Trp 111 (2.96 Å). These hydrogen bonds anchor the inhibitor in an anionic well deep within the enzyme active site. Interactions between the aromatic hydrophobic side chain of the inhibitor and apolar and aromatic residues lining the active sites further stabilize the inhibitors.

As this class of inhibitors bind to the ALR2 active site, a conformational change occurs opening a pocket between Trp 111 and Leu 300. The specific opening of the pocket varies to accommodate the particular inhibitor, producing an 'induced fit'. Since the residues lining this pocket are not conserved in ALR1, the interactions in this pocket are specific for ALR2. This is exemplified in Figure 3, where the structure of the complex ALR2—example **17** has been superposed with the structure of ALR1 (magenta). Using this superposed structure, it is clear that the inhibitor has strong steric clashes with the ALR1 residues Pro 301 (1.35 Å) and Tyr 116 (1.10 Å). These clashes can explain the strong selectivity of this class of inhibitors for ALR2 versus ALR1. The structure of example **17** has been deposited in the Protein Data Bank. The PDB code is 3G5E.

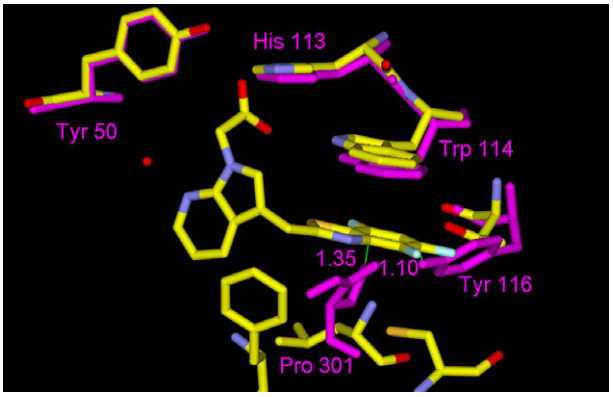

Figure 3.

Although it is not clear what selectivity profile is necessary to avoid potential aldehyde reductase related toxicity, combining the 4,5,7-trifluorobenzothiazole with novel heterocycle cores such as the 7-azaindole, can result is new ARIs with exceptional potency and selectivity.

Acknowledgments

This work was supported, in part, by the Centre National de la Recherche Scientifique (CNRS), the Institut National de la Santé et de la Recherche Médicale and the Hôpital Universitaire de Strasbourg (H.U.S.). We thank the personnel of the SBC, and in particular Andrzej Joachimiak and Ruslan Sanishvili (Nukro), for their help in data collection.

Supplementary data

Supplementary data associated with this article can be found, in the online version, at doi:10.1016/j.bmcl.2009.02.037.

References and notes

1. Lorenzi, M. *Exp. Diabetes Res.* **2007**, 61038.
2. (a) *Textbook of Diabetes*; Pickup, J. C., Williams, G., Eds.; Blackwell Science Ltd: United Kingdom, 1997; Vol. 1,. Chapter 42 (b) Williamson, J. R. et al *Diabetes* **1993**, *42*, 801; (c) Setter, S. M.; Campbell, R. K.; Cahoon, C. J. *Ann. Pharmacother.* **2003**, *37*, 1858; (d) Oates, P. J. *Curr. Drug Targets* **2008**, *9*, 14.
3. Ramirez, M. A.; Borja, N. L. *Pharmacotherapy* **2008**, *28*, 646.
4. Hamada, Y.; Nakamura, J. *Treatments Endocrinol.* **2004**, *3*, 245.
5. (a) Shinoda, M.; Mori, S.; Shintani, S.; Ishikura, S.; Hara, A. *Biol. Pharm. Bull.* **1999**, *22*, 741; (b) Suzuki, K.; Koh, Y. H.; Mizuno, H.; Hamaoka, R.; Taniguchi, N. *J. Biochem.* **1998**, *123*, 353; (c) Bodreddigari, S.; Jones, L. K.; Egner, P. A.; Groopman, J. D.; Sutter, C. H.; Roebuck, B. D.; Guengerich, F. P.; Kensler, T. W.; Sutter, T. R. *Chem. Res. Toxicol.* **2008**, *21*, 1134.
6. (a) Takahashi, M.; Fujii, J.; Teshima, T.; Suzuki, K.; Shiba, T.; Taniguchi, N. *Gene* **1993**, *127*, 249; (b) Kanazu, T.; Shinoda, M.; Nakayama, T.; Deyashiki, Y.; Hara, A.; Sawada, H. *Biochem. J.* **1991**, *279*, 903.
7. Hamada, Y.; Araki, N.; Koh, N.; Nakamura, J.; Horiuchi, S.; Hotta, N. *Biochem. Biophys. Res. Commun.* **1996**, *228*, 539.
8. (a) Oya, T.; Hattori, N.; Mizuno, Y.; Miyata, S.; Maeda, S.; Osawa, T.; Uchida, K. *J. Biol. Chem.* **1999**, *274*, 18492; (b) Cavalot, F.; Anfossi, G.; Russo, I.; Mularoni, E.; Massucco, P.; Mattiello, L.; Burzacca, S.; Hahn, A.; Trovati, M. *Metabolism* **1996**, *45*, 285; (c) Fu, M.; Wells-Knecht, K.; Blackledge, J.; Lyons, T.; Thorpe, S.; Baynes, J. *Diabetes* **1994**, *43*, 676.
9. Harrison, D. H. T.; Bohren, K. M.; Petsko, G. A.; Ringe, D.; Gabbay, K. H. *Biochemistry* **1997**, *36*, 16134.
10. (a) Van Zandt, M. C.; Jones, M. L.; Gunn, D.; Geraci, L. S.; Jones, J. H.; Sawicki, D. R.; Sredy, J.; Jacot, J. L.; DiCioccio, A. T.; Petrova, T.; Mitschler, A.; Podjarny, A. D. *J. Med. Chem.* **2005**, *48*, 3141; (b) Van Zandt, M. C.; Sibley, E. O.; McCann, E. E.; Combs, K. J.; Flam, B.; Sawicki, D.; Sabetta, A.; Carrington, A.; Sredy, J.; Howard, E.; Mitschler, A.; Chevrier, B.; Podjarny, A. *Bioorg. Med. Chem.* **2004**, *12*, 5661.
11. (a) El-Kabbani, O.; Podjarny, A. *Cell Mol. Life Sci.* **2007**, *15*, 1970; (b) Petrova, T.; Steuber, H.; Hazemann, I.; Cousido-Siah, A.; Mitschler, A.; Chung, R.; Oka, M.; Klebe, G.; El-Kabbani, O.; Joachimiak, A.; Podjarney, A. *J. Med. Chem.* **2005**, *18*, 5659.